Angular differential studies of electron transfer in collisions of He-like ions with Na(3*s*): The role of electron saddle crossings

I. Blank,[1] S. Otranto,[2] C. Meinema,[1] R. E. Olson,[3] and R. Hoekstra[1]
[1]*KVI, Atomic Physics, University of Groningen, NL-9747 AA, Groningen, The Netherlands*
[2]*Departamento de Física, Universidad Nacional del Sur, 8000 Bahía Blanca, Argentina*
[3]*Physics Department, Missouri University of Science and Technology, Rolla, Missouri 65409, USA*
(Received 19 November 2012; published 20 March 2013)

We present a systematic experimental and theoretical study of angular differential cross sections of single-electron transfer in collisions of N^{5+}, O^{6+}, and Ne^{8+} with ground-state Na(3*s*) in the collision energy range from 1 to 8 keV/amu. Experiments were performed using recoil-ion momentum spectroscopy in combination with a magneto-optically cooled Na atom target. The results are compared with three-body classical-trajectory Monte Carlo theory. Experimental and theoretical angular differential cross sections for capture into highly excited states show an oscillatory structure which is linked to the number of times the active electron crosses the potential energy saddle, i.e., oscillates between the two nuclear centers during the collision process.

DOI: 10.1103/PhysRevA.87.032712 PACS number(s): 34.70.+e

I. INTRODUCTION

Electron transfer in collisions of highly charged ions with atoms is the dominant process in the low-keV/amu collision energy range and as such has been studied extensively both theoretically and experimentally; see, e.g., [1,2]. As for total charge exchange cross sections in general there is excellent agreement between theory and experiment. On the level of state-selective one-electron capture the comparison between theory and experiment is usually very satisfactory as well. To understand the underlying dynamics of electron transfer processes and to test theory on the most basic level, angular differential measurements are required. Charge transfer in collisions of highly charged ions with atoms occurs at large impact parameters, leading to very small projectile scattering angles in the order of 0.1 mrad. With the development of recoil-ion momentum spectroscopy (RIMS) it became possible to obtain angular differential charge transfer information with hitherto unprecedented resolution with nearly 4π solid-angle detection efficiency [3,4]. To take advantage of the increased resolution RIMS requires a cold target such as supersonic gas jets or laser-cooled atoms.

We present experimental and theoretical state-selective differential cross sections for electron transfer in collisions of highly charged He-like ions (N^{5+}, O^{6+}, and Ne^{8+}) with Na(3*s*). Experimental differential cross sections are extracted from Na^+ recoil spectra obtained using the MOTRIMS technique [5–7] which combines RIMS with a target that is laser cooled and trapped in a magneto-optical trap (MOT). The results are compared with those from three-body classical-trajectory Monte Carlo (CTMC) theory [8]. Since electron transfer in ion-atom collisions involving highly charged ions lead to population of highly excited final states, the CMTC framework is ideally suited to study these systems as it is not limited by a finite basis set. Calculations of the transition probability as a function of the impact parameter give additional insight into the electron transfer dynamics.

In the present study we show that the active electron can be transferred from the target to the projectile in one direct step, or can cross the potential barrier between the projectile and the target nuclear centers several times. While the effect of these electron oscillations is washed out in the total cross sections, structures resulting from the different numbers of times the electron crosses the potential saddle point appear in both the state-selective cross sections and, more strongly pronounced, in the angular differential spectra for capture into highly excited states.

Similar features have been reported for total capture cross sections in slow symmetric and inelastic alkali-metal ion-atom collisions [9], state-selective capture cross sections from Rydberg-state atoms [10], electron excitation cross sections [11], and electron transfer probabilities as a function of the impact parameter in collisions of slow Na^+ with Rb [12].

Oscillations on angular differential cross sections for symmetric ion-atom systems have been reported in the pioneering work from Everhart *et al.* [13]. An explanation for the oscillations was provided by Marchi and Smith [14] as related to the detailed measurements by Aberth *et al.* for the $He^+ + He$ system [15]. The Marchi and Smith work was extended to asymmetric ion-atom collisions where the oscillatory structure was sometimes termed "Stueckelberg oscillations" [16]. Another example where oscillatory structure in angular differential cross sections has been explained in terms of such Stueckelberg oscillations has been presented in Ref. [17] for two-electron transfer in $C^{4+} + He$ collisions. In all of the above studies and those to date (see Sec. 4.4.2.4 of the review [18]), the oscillations were described following the premise that the particles follow a limited number (usually two) of different trajectories within the interaction region that are each associated with different quantal phases. The oscillatory angular cross sections arise from the interference of these phases. In the studies presented here, the number of product states associated with the various high (n,l) levels are in the hundreds so that it is difficult to ascribe oscillatory structure to specific state-to-state phase interference effects. Moreover, our CTMC calculations carry no phase information within them. Thus, a simpler explanation based on the number of times the active electron moves between nuclear centers is invoked and is found to qualitatively reproduce the data.

In a preceding paper by Otranto *et al.* [19] we showed that electron oscillations play a major role in $Ne^{8+} + Na(3s)$ capture collisions. In this work we extend our previous results

and show that such structures are also present in spectra resulting from collisions of $N^{5+} + Na(3s)$ and $O^{6+} + Na(3s)$. Since we observe the electron oscillations in three different systems of collisions of highly charged ions with $Na(3s)$ and considering previous findings by other groups this process appears to be general feature of ion-atom collisions.

This paper is organized as follows: The experimental setup and data acquisition are described in Sec. II. An overview of the CMTC method is given in Sec. III. Experimental and theoretical angular differential spectra are presented in Sec. IV. The dynamics of the collision systems is discussed in Sec. V. Finally, we give our conclusions in Sec. VI. Atomic units are used throughout the paper, unless stated otherwise.

II. EXPERIMENTAL METHOD

Our MOTRIMS apparatus has been described elsewhere [20]. In short the ^{23}Na target atoms are cooled and trapped in a magneto-optical trap. The ion beam provided by our electron cyclotron resonance ion source is collimated to about 1 mm and crossed with the target atom cloud. The Na^+ recoil ions created in collisions involving electron transfer are extracted transverse to the ion beam direction by a low electric field (0.4 V/cm to 2 V/cm) towards the detector where their two-dimensional position is recorded. From these data the recoil-momentum vector can be reconstructed. Higher extraction values are used at low collision energies where the resulting repulsion between projectile and recoil ion leads to large recoil momenta. The Q value of the process, i.e., the total change of binding energies of all electrons before and after the collision, is related to the longitudinal momentum of the recoil ions by

$$p_{\text{long}} = \frac{Q}{v_p} - \frac{1}{2} r v_p. \tag{1}$$

Here v_p is the projectile-ion velocity and r is the number of transferred electrons. Since the initial binding energies of the collision partners are well known, the Q value directly yields the final-state distribution of the transferred electrons in the projectile.

During standard operation the atomic sample in a MOT contains a mixture of ground- and excited-state atoms. For experiments with ground-state $Na(3s)$ all laser beams of the MOT are switched off using an acousto-optical modulator (AOM) with a frequency of about 7 kHz and a duty cycle of 66%. The measurements are performed with a continuous ion beam. Application of a timing gate on the detector synchronized to the AOM switching frequency ensures that all target atoms have decayed to the ground state before the collision. This is possible due to the much shorter decay time of the excited $Na^*(3p)$ with respect to the AOM switching frequency.

The transverse momentum component of the recoil-ion momentum vector is directly proportional to the projectile's scattering angle θ via the relation

$$p_{\text{trans}} = m_P v_P \theta, \tag{2}$$

where m_P is the projectile's mass and v_P is its velocity. The transverse momentum is a two-dimensional vector with the magnitude $p_{\text{trans}} = (p_y^2 + p_z^2)^{1/2}$ and in our case the p_y component is related to the recoil's position on the detector while the p_z component corresponds to the recoil's time of flight in the spectrometer. State-selective angular differential cross sections are obtained by restricting the longitudinal momentum component to Q values corresponding to capture into a specific final state.

Although in principle it would be possible to obtain both transverse momentum components experimentally, it is in fact necessary to measure only one component. Due to the cylindrical symmetry of the system the Abel inversion can be applied to obtain the full transverse momentum distribution from the projection onto one of the transverse momentum axes [21]. We chose the latter approach, which allowed us to measure several events per laser on-off cycle. Since the bin size of the detector is smaller than the experimental resolution each bin contains statistical noise. The Abel inversion procedure is very sensitive to fluctuations in the input distribution and tends to amplify noise greatly. Thus it is necessary to apply a smoothing procedure to the data before performing the Abel inversion, which results in smooth transverse momentum spectra.

To verify the validity of this procedure we performed a measurement with a pulsed 3 keV/amu N^{5+} beam which was used as a start signal to obtain the transverse momentum from the time of flight as well. The resulting Na^+ recoil distribution is shown in Fig. 1. Separate contributions in the spectrum resulting from electron capture into final states $N^{4+}(n)$, $n = 5$, 6, and 7, are indicated. Since a Na MOT also produces sodium molecular ions $Na_2{}^+$ by associative ionization of excited Na atoms [22,23], they are recorded in the recoil spectra as well. A comparison of the directly measured transverse momentum distribution and the corresponding spectrum obtained by applying the Abel inversion on the projection of the spectrum onto the p_y component for the final state $N^{4+}(n = 7)$ is shown in Fig. 2. The good agreement between the two methods confirms our data acquisition and analysis procedure.

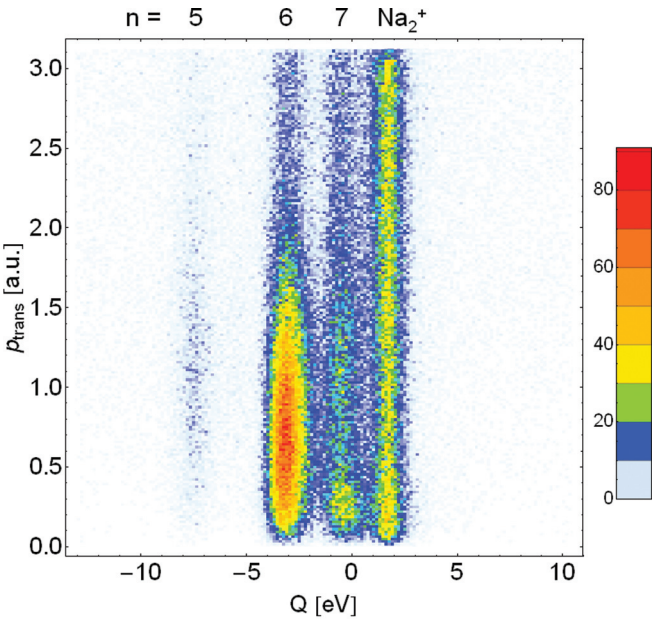

FIG. 1. (Color online) Transverse momentum vs Q value spectrum of Na^+ recoils obtained with a pulsed 3 keV/amu N^{5+} ion beam colliding with $Na(3s)$. The final states of the electron in the target as well as the contribution of $Na_2{}^+$ molecular ions are indicated.

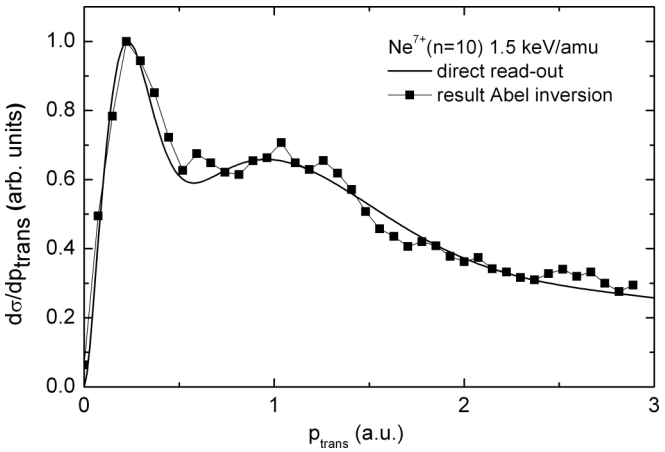

FIG. 2. Comparison of the direct measurement of the transverse momentum of Na^+ recoils resulting from $N^{5+} + Na(3s) \rightarrow N^{4+}$ $(n = 7) + Na^+$ collisions and the corresponding result obtained by applying the Abel inversion on the projection onto the p_y momentum component.

The momentum resolution in the p_{long} direction is estimated at 0.05 a.u. from the width of the $Na_2{}^+$ molecular ion peak. Due to the reconstruction procedure the resolution of the transverse momentum spectra is estimated at 0.2 a.u. Figure 3 shows a comparison of experimental and CTMC transverse momentum spectra with and without convolution for $Ne^7(n = 10)$. While there is qualitative agreement between the experimental and CTMC spectra, the quantitative agreement improves when the CTMC transverse momentum spectrum is convoluted with a Gaussian with a width of 0.2 a.u.

III. THEORETICAL METHOD

Theoretical single-electron capture and ionization cross sections have been calculated using the CTMC method [8]. Hamilton's equations are solved for a mutually interacting three-body system. To mimic the experimental conditions, the center of mass of the Na target is frozen at the beginning of each simulation. The active electron evolves under the central-potential model developed by Green *et al*. from Hartree-Fock calculations [24], and later generalized by Garvey *et al*. [25].

The CTMC method is not limited by basis-set size for the prediction of capture to very high-lying excited states. We note that the electron tends to be captured to high n values and the orbital energies are similar to those obtained with bare projectiles. Hence, we represent the captured electron-projectile interaction by a Coulomb potential where the projectile's asymptotic charge is considered. A classical number n_c is obtained from the binding energy E_p of the electron relative to the projectile by

$$E_P = -Z_P^2/(2n_c^2), \tag{3}$$

where Z_p is the charge of the projectile core. Then n_c is related to the principal quantum number n of the final state by the condition derived by Becker and McKellar [26]:

$$\left[(n-1)\left(n-\tfrac{1}{2}\right)n\right]^{1/3} \leqslant n_c \leqslant \left[n(n+1)\left(n+\tfrac{1}{2}\right)\right]^{1/3}. \tag{4}$$

The latter provides a final-state binning for n_c such that the phase-space volume per bin equals the multiplicity n^2 of the quantal n shell.

The cross section for a definite n state is then given by

$$\sigma_n = N(n)\pi b_{\max}^2/N_{\text{tot}}, \tag{5}$$

where $N(n)$ is the number of events of electron capture to the n level and N_{tot} is the total number of trajectories integrated. The impact parameter $b_{\max}$ is the value beyond which the probability of electron capture is negligibly small.

Since all two-body interactions are included in the CTMC calculations, it is possible to calculate the recoil transverse momentum cross sections differential in the product n level.

Furthermore, an electron saddle crossing is recorded in the CTMC code each time the component of the electron position vector $\mathbf{r}_e$ along the internuclear axis ($\mathbf{r}_e \cdot \mathbf{R}$) crosses the potential saddle position r_{saddle} which is a function of the internuclear distance $\mathbf{R}$. Once the electron's energy overcomes the potential barrier it can move in the field of both ions. The interaction time is inversely proportional to the collision energy, which implies more saddle crossings with decreasing projectile velocities.

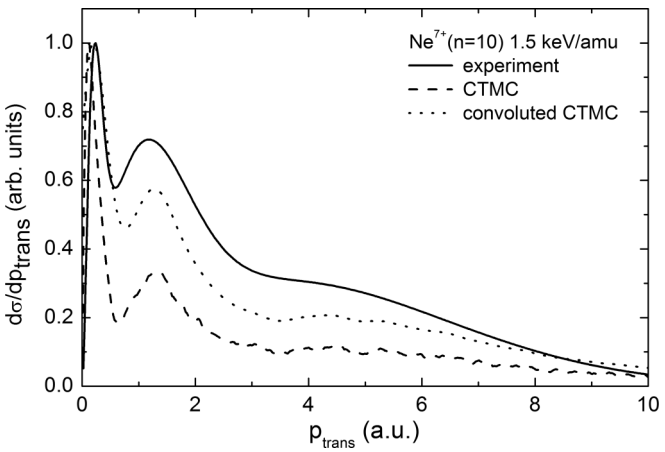

FIG. 3. Comparison of transverse momentum spectra of Na^+ recoils from $Ne^{8+} + Na(3s) \rightarrow Ne^{7+}(n = 10) + Na^+$: experimental and CTMC results with and without convolution.

IV. RESULTS

Experimental Q value spectra of Na^+ recoil ions resulting from electron transfer in collisions of N^{5+}, O^{6+}, and Ne^{8+} with $Na(3s)$ at a collision energy of 2 keV/amu are shown in Fig. 4. At low keV/amu energies electron transfer is known to be very selective with respect to the electron final state in the projectile. At 2 keV/amu capture into the dominant final states $N^{4+}(n = 6)$, $O^{5+}(n = 7)$, and $Ne^{7+}(n = 9)$ accounts for over 50% of the relative cross section for each presented system. With increasing collision energy, electron transfer into higher final states takes on greater significance and there is a marked increase of the ionization cross section. A more detailed depiction of the energy dependence of the cross sections has been reported in Ref. [27] for the system $O^{6+} + Na(3s)$ and [20] for the systems $N^{5+} + Na(3s)$ and $Ne^{8+} + Na(3s)$.

Figure 5 shows experimental and theoretical transverse momentum distributions for capture into the dominant final states $N^{4+}(n = 6)$, $O^{5+}(n = 7)$, and $Ne^{7+}(n = 9)$ at 2 keV/amu

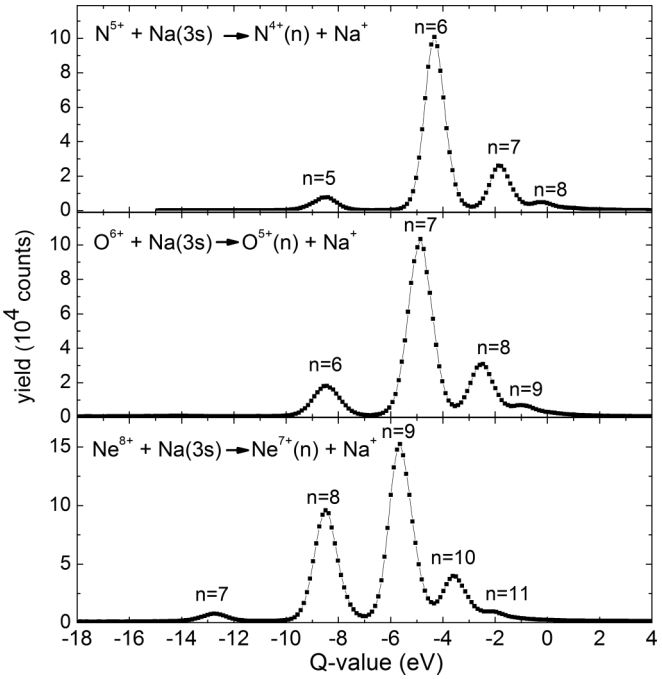

FIG. 4. Experimental Q value distributions of Na^+ recoil ions resulting from collisions of N^{5+}, O^{6+}, and Ne^{8+} with Na($3s$) at 2 keV/amu. The final states of the electron in the projectile are indicated.

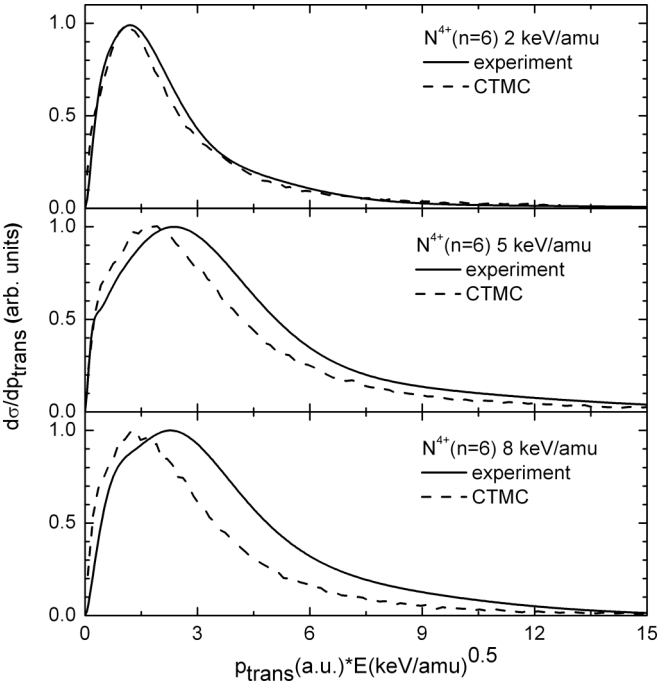

FIG. 6. Experimental and CTMC recoil-ion transverse momentum spectra for the process $N^{5+} + Na(3s) \rightarrow N^{4+}(n = 6) + Na^+$ at 2, 5, and 8 keV/amu projectile energy.

for N^{5+} and Ne^{8+} and 2.25 keV/amu for O^{6+}. For easy comparison all transverse momentum spectra are normalized to a peak value of 1. All experimental spectra show just one maximum around a transverse momentum of 1 a.u., which for O^{6+} corresponds to a projectile scattering angle of 0.12 mrad. The maxima are located at slightly smaller momenta for N^{5+} and somewhat larger momenta for Ne^{8+}. All distributions smoothly extend to higher momenta, up to 5 a.u. for N^{5+} and up to 7 a.u. for Ne^{8+} projectiles. The shift to larger momenta for higher projectile charge is a direct result of the increased repulsion of the projectile ion and the resulting recoil ion. The agreement between experimental and CTMC results is very good.

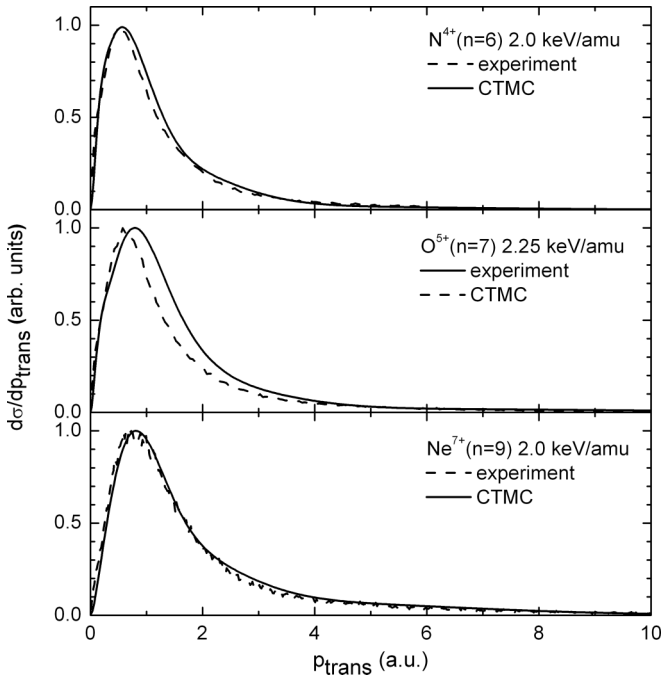

FIG. 5. Experimental and CTMC recoil-ion transverse momentum spectra for the respective dominant capture channel in collisions of N^{5+}, O^{6+}, and Ne^{8+} with Na($3s$) at 2 and 2.25 keV/amu, respectively.

To illustrate the collision energy dependence of this process, transverse momentum spectra for capture into $N^{4+}(n = 6)$ at 2, 5, and 8 keV/amu are shown in Fig. 6. In order to compare transverse momentum spectra at different collision energies the abscissa is multiplied by the square root of the projectile energy. Under the assumption of pure Rutherford scattering, this should remove the collision energy dependence resulting from a change of the interaction time. The resulting transverse momentum spectra show a trend to higher momentum values with increasing collision energy. Since in this representation the abscissa is approximately inversely proportional to the impact parameter this implies that the electron transfer process shifts to smaller impact parameters with increasing collision energy. Figure 7 shows the weighted CTMC transition probabilities for the final state $N^{4+}(n = 6)$ at 2, 5, and 8 keV/amu. The trend to smaller impact parameters with increasing collision energy is clearly shown. This can be explained by the increasing importance of capture into higher final states at higher collision energies which draw flux at large impact parameters. Similarly to the experimental and theoretical transverse momentum spectra the CTMC transition probabilities show only one distinct maximum over the whole collision energy range.

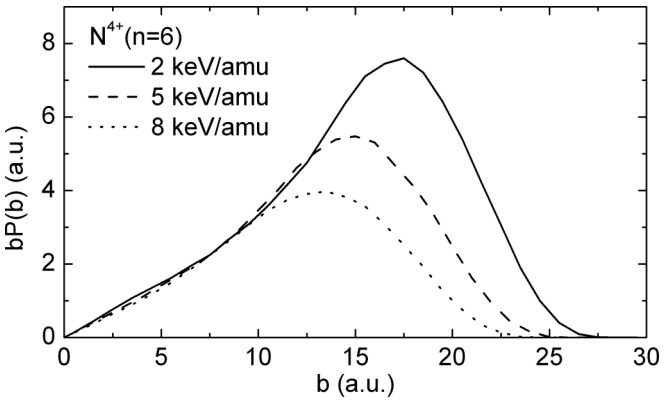

FIG. 7. Weighted CTMC electron capture transition probabilities as a function of the impact parameter b for capture into the $N^{4+}(n = 6)$ final state at 2, 5, and 8 keV/amu.

For the next higher final n shells $N^{4+}(n = 7)$, $O^{5+}(n = 8)$, and $Ne^{7+}(n = 10)$, experimental and CTMC transverse momentum spectra obtained at 2 keV/amu for N^{5+} and Ne^{8+} and 2.25 keV/amu for O^{6+} are shown in Fig. 8. Though there is some quantitative discrepancy between theory and experiment, the experimentally observed structure in the spectra is well reproduced by the CTMC calculations. The quantitative discrepancy between experiment and CTMC can be largely attributed to the insufficient experimental resolution, as discussed in Sec. II. The experimental spectra show a pronounced maximum at very low momenta around 0.2 a.u. for all projectile ions, which corresponds to a projectile scattering angle of only 0.02 mrad for O^{6+} projectiles, and a second maximum at momenta between 1 and 2 a.u. The spectra extend to high momentum values of up to 8 a.u., which is further than

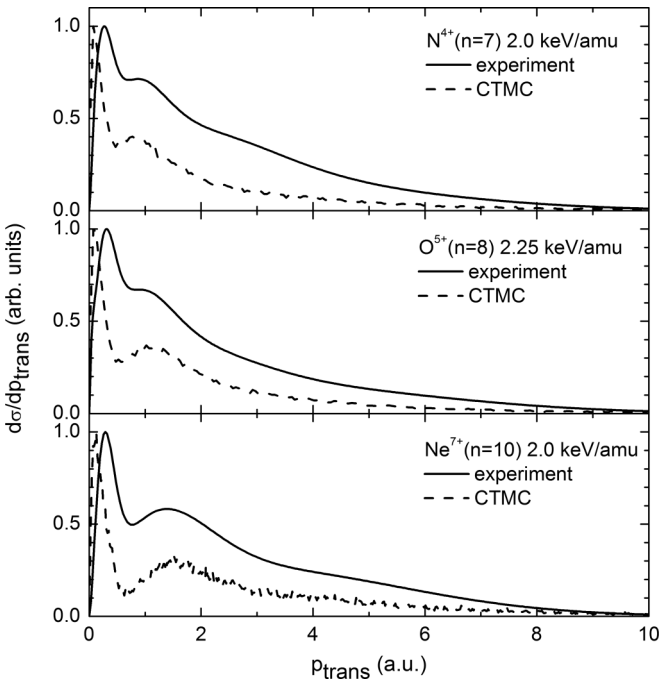

FIG. 8. Experimental and CTMC recoil-ion transverse momentum spectra for the final states $N^{4+}(n = 7)$, $O^{5+}(n = 8)$, and $Ne^{7+}(n = 10)$ at 2 and 2.25 keV/amu, respectively.

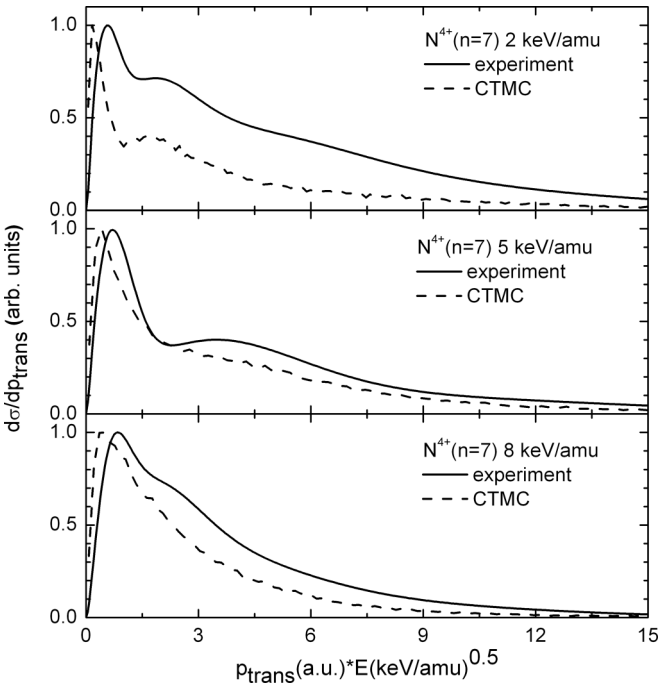

FIG. 9. Experimental and CTMC transverse momentum spectra for the process $N^{5+} + Na(3s) \rightarrow N^{4+}(n = 7) + Na^{+}$ at 2, 5, and 8 keV/amu.

for the corresponding main capture channel, indicating capture events at very small impact parameters.

As an exemplary case a comparison of the CTMC and experimental spectra for $N^{5+} + Na(3s) \rightarrow N^{4+}(n = 7) + Na^{+}$ collisions at 2, 5, and 8 keV/amu is shown in Fig. 9. Although again there is some quantitative discrepancy between theory and experiment, the qualitative agreement with regard to the change of the shape of the spectrum as a function of collision energy is rather satisfactory. While at 8 and 5 keV/amu the oscillatory structure is only very weakly hinted at, it becomes apparent at a collision energy of 2 keV/amu. Corresponding weighted CTMC transition probabilities as a function of the impact parameter for the $N^{4+}(n = 7)$ final state at 2, 5, and 8 keV/amu are shown in Fig. 10. With increasing collision energy the capture probability into $N^{4+}(n = 7)$ increases at

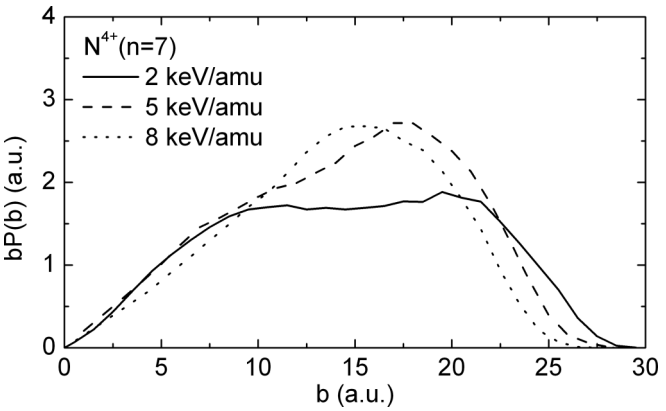

FIG. 10. Weighted CTMC electron capture transition probabilities as a function of the impact parameter b for capture into the $N^{4+}(n = 7)$ final state at 2, 5, and 8 keV/amu.

larger impact parameter between 10 and 22 a.u. at the expense of the $N^{4+}(n = 6)$ final state as has been shown in Fig. 7.

V. DISCUSSION

Since the transverse momentum spectra obtained with the different projectile ions show similar features, we will consider the $N^{5+} + Na(3s)$ system as an exemplary case. A discussion of transverse momentum spectra for the system $Ne^{8+} + Na(3s)$ has been presented in Ref. [19]. To explain the origin of the structure seen in the differential cross sections, CTMC calculations have been performed which monitored how many times the active electron crosses the barrier, i.e., oscillates, between the target and the projectile. In the case of electron transfer the electron has to cross the saddle an odd number of times from the target to the projectile.

A comparison between experimental and CTMC transverse momentum distributions for the processes $N^{5+} + Na(3s) \rightarrow N^{4+}(n) + Na^{+}$ for $n = 6$ and $n = 7$ at 2 keV/amu collision energy is presented in Fig. 11, explicitly showing the contributions of the different number of times the electron crosses the barrier. Here, the experimental data are put on an absolute scale using the theoretical maximum values. Even though the transverse momentum spectrum for the $N^{4+}(n = 6)$ final state shows no structure, the CTMC calculations reveal that the spectrum consists of contributions of different numbers of electron saddle crossings. Direct transfer, i.e., one crossing, leads to final transverse momenta between 0 and 3 a.u., maximizing at about 0.5 a.u. From 1 a.u. on the contribution of three crossings starts to rise, with a maximum at about 1.8 a.u. At this collision energy contributions of five and more crossings play only a very minor role. The contributions of different numbers of electron saddle crossings to the spectrum are overlapping to a smooth total distribution without additional structures.

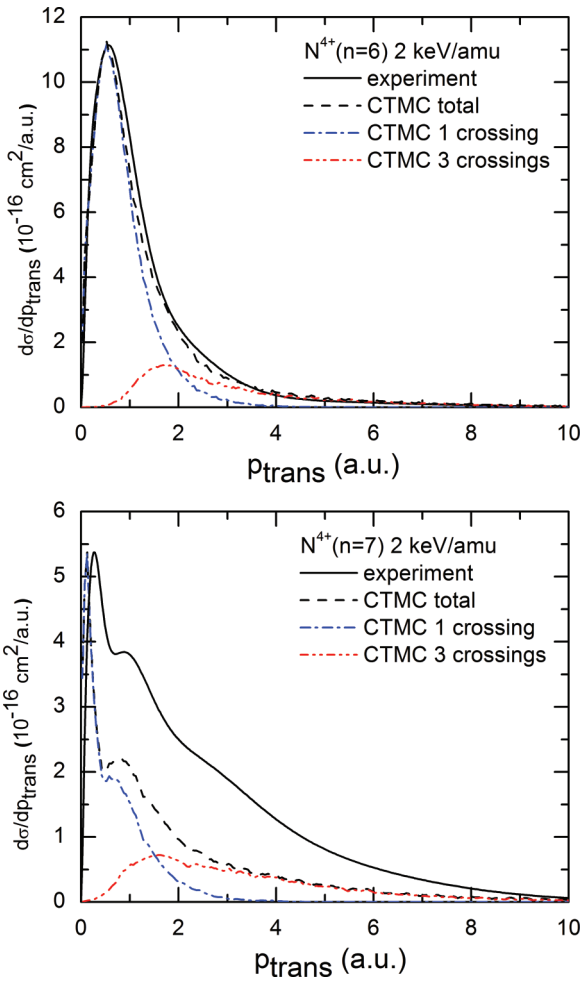

FIG. 11. (Color online) Transverse momentum distributions for the processes $N^{5+} + Na(3s) \rightarrow N^{4+}(n) + Na^{+}$ for $n = 6$ and $n = 7$ at 2.0 keV/amu.

The transverse momentum spectrum for the $N^{4+}(n = 7)$ final state is comprised of mainly the contributions of one and three crossings as well. The main difference for the $N^{4+}(n = 7)$ final state manifests itself in the one-crossing contribution, which shows a sharp peak at small transverse momenta around 0.2 a.u. and a second peak at about 1 a.u., so that the resulting total spectrum retains some of the structure resulting from the two processes.

It has been found that transverse momentum spectra for the systems $Ne^{8+} + Na(3s)$ [19] and $O^{6+} + Na(3s)$ (not shown) can be interpreted in terms of events of different numbers of electron saddle crossings as well. In general, electron capture after just one crossing leads to small transverse momenta ($\lesssim$1 a.u.), whereas the contributions at larger momenta ($\gtrsim$1 a.u.) are due to events of three or more saddle crossings.

Figure 12 shows the weighted CTMC transition probabilities as a function of the impact parameter b, explicitly indicating the contributions arising from different numbers of electron saddle crossings for collisions of 2 keV/amu N^{5+} with $Na(3s)$. For the $N^{4+}(n = 6)$ final state, one-step transfer occurs

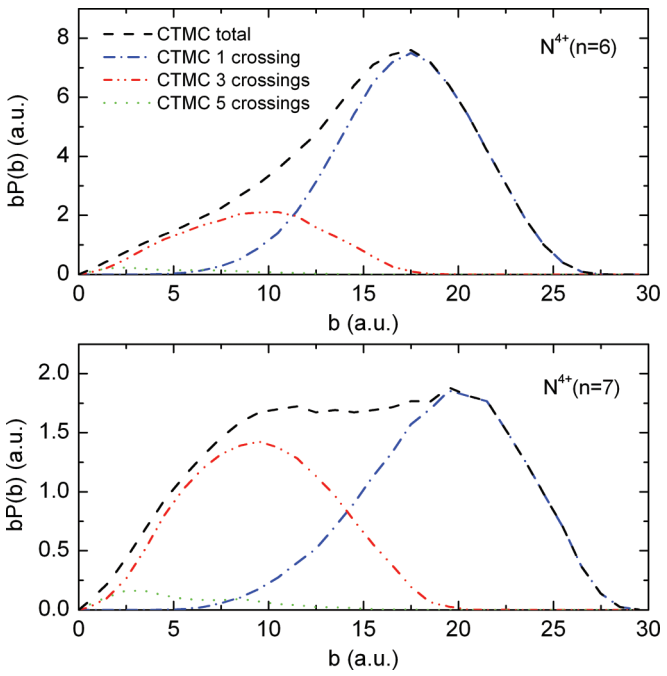

FIG. 12. (Color online) Weighted CTMC electron transfer probability distributions for the process $N^{5+} + Na(3s) \rightarrow N^{4+}(n) + Na^{+}$, $n = 6$ and 7, at 2 keV/amu. Contributions arising from different numbers of electron saddle crossings are explicitly shown.

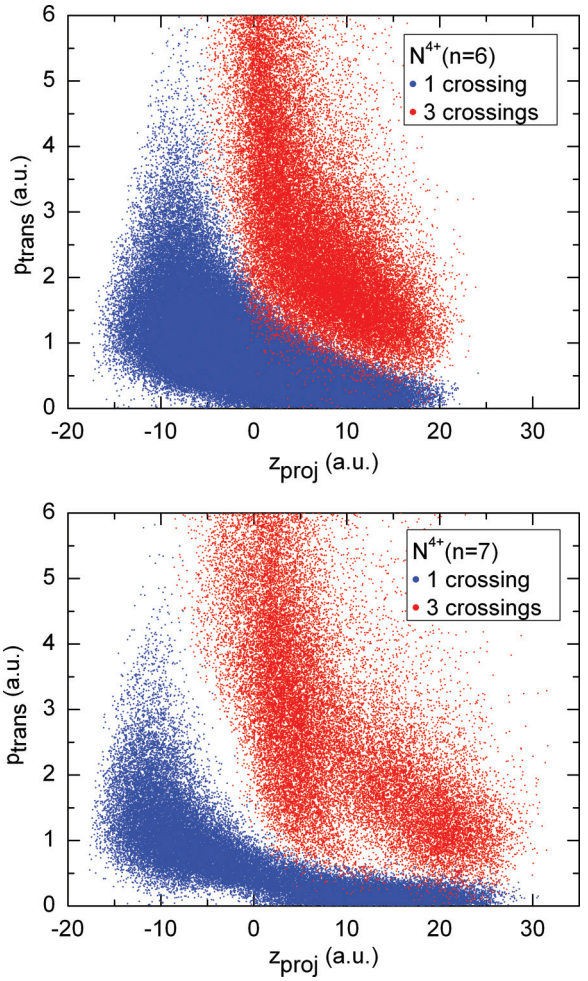

FIG. 13. (Color online) Final CTMC transverse momentum versus the position of the projectile with respect to the target (z_{proj}) at the last saddle crossing for $N^{5+} + Na(3s) \rightarrow N^{4+}(n) + Na^{+}$ for $n = 6$ and $n = 7$ at 2.0 keV/amu.

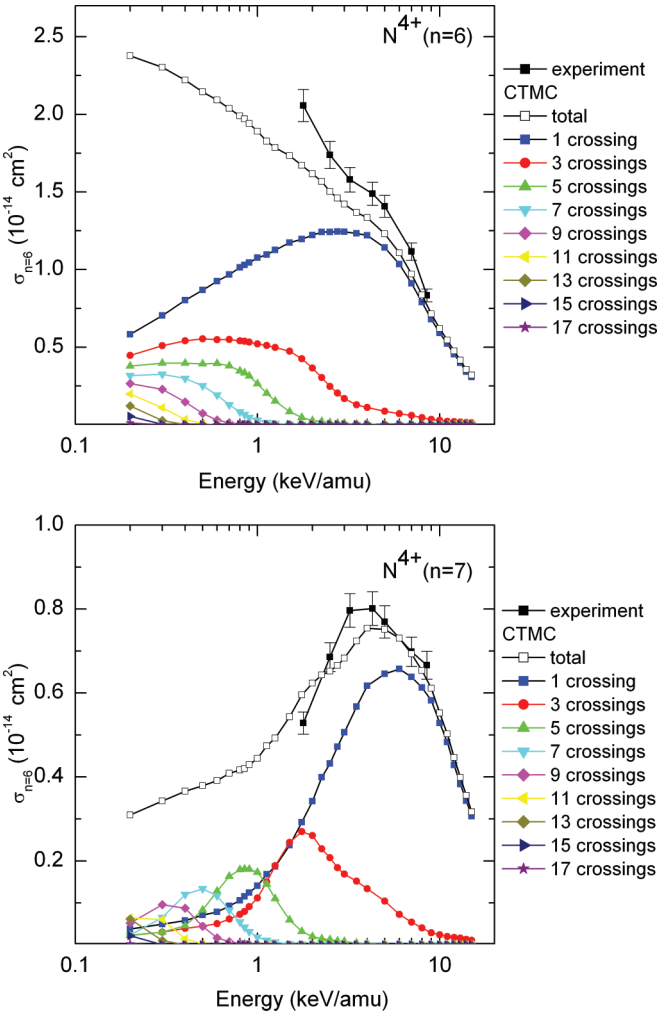

FIG. 14. (Color online) Electron transfer cross sections for the process $N^{5+} + Na(3s) \rightarrow N^{4+}(n) + Na^{+}$, $n = 6$ and $n = 7$, as a function of collision energy. The partial contributions arising from different numbers of electron saddle crossings are explicitly shown.

over a broad range of impact parameters from 7 to 25 a.u., maximizing at about 16 a.u. At smaller impact parameters below 15 a.u. the process involving three saddle crossings gains in importance and dominates the collision dynamics at impact parameters below 10 a.u. At very low impact parameters below 5 a.u. a very weak contribution of five saddle crossings transfer appears as well. The increasing importance of the number of electron saddle crossings with decreasing impact parameter can be understood by the increasing interaction time of projectile and target at smaller impact parameters. Comparing the transition probabilities for the $N^{4+}(n = 6)$ and $N^{4+}(n = 7)$ final states, the capture processes involving different numbers of electron crossings occur at similar impact parameters. However while for the $N^{4+}(n = 6)$ final state the direct transfer mechanism dominates, the $N^{4+}(n = 7)$ final state is populated almost equally via one and three saddle crossing processes. The increasing importance of more electron crossings for higher excited final states can be explained by the increasing interaction time as well.

For further investigation of the collision dynamics distributions of CTMC events differential in transverse momentum and the position of the projectile with respect to the target z_{proj} at which the active electron crosses the barrier to the projectile for the final time is shown in Fig. 13. In this representation $z_{\mathrm{proj}} = 0$ is the point where the projectile passes the target. For the final states $N^{4+}(n = 6)$ and $N^{4+}(n = 7)$ a direct transfer of the electron, i.e., one crossing, can occur over a large z_{proj} range on the incoming and outgoing parts of the projectile trajectory. If the electron is transferred on the incoming path ($z_{\mathrm{proj}} < 0$) the resulting transverse momentum is rather large, in the range of several a.u. If the electron is transferred on the outgoing trajectory ($z_{\mathrm{proj}} > 0$) the resulting transverse momentum is quite small. For capture into $N^{7+}(n = 6)$ the one-crossing capture events are smoothly spread out over the whole p_{trans}-z_{proj} range, so that there is no distinction between capture events on the incoming or outgoing part of the projectile trajectory, which leads to a single large, broad peak in the projection onto p_{trans}. On the other hand the structure seen in the transverse momentum spectrum of one-crossing capture into the $N^{4+}(n = 7)$ final state can be attributed to either capture on the incoming ($p_{\mathrm{trans}} > 0.5$ a.u.) or outgoing ($p_{\mathrm{trans}} < 0.5$ a.u.) part of the projectile trajectory. While direct

electron transfer can happen during both the incoming and outgoing parts of the projectile trajectory, final capture of the electron after three saddle crossings occurs almost exclusively on the outgoing part ($z_{\mathrm{proj}} > 0$) for both final states $N^{4+}(n = 6)$ and $N^{4+}(n = 7)$. In $Ne^{8+} + Na(3s)$ collisions, final capture in events involving three electron saddle crossings has been found to take place in either the incoming or outgoing parts of the projectile trajectory [19]. In contrast, the present data for N^{5+} suggest that these are restricted to the outgoing part only, highlighting a possible dependence of these mechanisms on the asymptotic projectile charge. Comparing the final transverse momentum at one z_{proj} value, it becomes apparent that electron transfer involving three or more saddle crossings leads to larger momenta. This is caused by the preceding bouncing of the electron between the ionic centers, which reduces the screening of the target charge and thus causes a larger repulsion of target and projectile, leading to larger final transverse momenta.

To illustrate the collision energy dependence of the electron saddle crossings a comparison of the experimental and CTMC cross sections for capture into $N^{4+}(n = 6)$ and $N^{4+}(n = 7)$ final state is shown in Fig. 14 with explicit contributions of the different numbers of crossings. The experimental relative cross sections are put on an absolute scale using CMTC total cross sections. For the $N^{4+}(n = 6)$ final state the one-crossing contribution shows a maximum at about 4 keV/amu and is the dominant process over the whole theoretically investigated energy range from 0.2 to 10 keV/amu. With decreasing collision energy, contributions from three and more crossings become more relevant, although the increase is only gradual and the different contributions show only weakly pronounced maxima. For the $N^{4+}(n = 7)$ final state the one-crossing contribution has a pronounced maximum at about 6 keV/amu and decreases very rapidly with decreasing collision energy in favor of the three-crossing contribution, which starts to dominate the collision dynamics at 2 keV/amu. At even lower collision energies below 1 keV/amu, contributions of five or more crossings start to successively gain in importance and dominate the transfer dynamics. The increase in the number of electron saddle crossings with decreasing collision energy is directly linked to the longer interaction time of target and projectile, allowing for more electron oscillations.

VI. CONCLUSIONS

In summary, we have obtained experimental transverse momentum distributions in collisions of highly charged N^{5+}, O^{6+}, and Ne^{8+} ions with ground-state $Na(3s)$ in the collision energy range from 1 to 8 keV/amu. The results are compared with classical trajectory Monte Carlo calculations which are in general in a qualitatively good agreement with the experimental data. We find that the structure in the transverse momentum spectra observed for capture into higher final states can be explained in terms of the number of times the active electron crosses the barrier between the target and the projectile during the collision process. The CTMC calculations show that direct electron transfer can happen during both the incoming and outgoing parts of the projectile trajectory. Final capture of the electron event involving three electron saddle crossings appears almost exclusively on the outgoing part. The significance of electron saddle crossings strongly increases with decreasing collision energy, which has been found to be a general feature of all investigated collision systems.

ACKNOWLEDGMENTS

Work at KVI is sponsored by the Helmholtzzentrum für Schwerionenforschung GmbH (GSI), Germany–KVI University of Groningen Collaboration Agreement. Work at UNS was supported by Grant No. PGI 24/F049 and Grant No. PIP 112-200801-02760 of CONICET (Argentina).

[1] R. K. Janev and H. Winter, Phys. Rep. **117**, 265 (1985).
[2] W. Fritsch and C. D. Lin, Phys. Rep. **202**, 1 (1991).
[3] J. Ullrich, R. Moshammer, R. Dörner, O. Jagutzki, V. Mergel, H. Schmidt-Böcking, and L. Spielberger, J. Phys. B **30**, 2917 (1997).
[4] R. Dörner, V. Mergel, O. Jagutzki, L. Spielberger, J. Ullrich, R. Moshammer, and H. Schmidt-Böcking, Phys. Rep. **330**, 95 (2000).
[5] M. van der Poel, C. V. Nielsen, M.-A. Gearba, and N. Andersen, Phys. Rev. Lett. **87**, 123201 (2001).
[6] J. W. Turkstra, R. Hoekstra, S. Knoop, D. Meyer, R. Morgenstern, and R. E. Olson, Phys. Rev. Lett. **87**, 123202 (2001).
[7] X. Fléchard, H. Nguyen, E. Wells, I. Ben-Itzhak, and B. D. DePaola, Phys. Rev. Lett. **87**, 123203 (2001).
[8] R. E. Olson and A. Salop, Phys. Rev. A **16**, 531 (1977).
[9] J. Perel, R. H. Vernon, and H. L. Daley, Phys. Rev. **138**, A937 (1965).
[10] K. B. MacAdam, J. C. Day, J. C. Aguilar, D. M. Homan, A. D. MacKellar, and M. J. Cavagnero, Phys. Rev. Lett. **75**, 1723 (1995).
[11] D. R. Schultz, C. O. Reinhold, and P. S. Krstić, Phys. Rev. Lett. **78**, 2720 (1997).
[12] A. Leredde, A. Cassimi, X. Fléchard, D. Hennecart, H. Jouin, and B. Pons, Phys. Rev. A **85**, 032710 (2012).
[13] G. J. Lockwood, H. F. Helbig, and E. Everhart, Phys. Rev. **132**, 2078 (1963).
[14] R. P. Marchi and F. T. Smith, Phys. Rev. **139**, A1025 (1965).
[15] W. Aberth, D. C. Lorents, R. P. Marchi, and F. T. Smith, Phys. Rev. Lett. **14**, 776 (1965).
[16] R. E. Olson and F. T. Smith, Phys. Rev. A **3**, 1607 (1971).
[17] A. Barany, H. Danared, H. Cederquist, P. Hvelplund, H. Knudsen, J. O. K. Pedersen, C. L. Cocke, L. N. Tunnell, W. Waggoner, and J. P. Giese, J. Phys. B **19**, L427 (1986).
[18] C. Cocke and R. Olson, Phys. Rep. **205**, 153 (1991).

[19] S. Otranto, I. Blank, R. E. Olson, and R. Hoekstra, J. Phys. B **45**, 175201 (2012).
[20] I. Blank, S. Otranto, C. Meinema, R. E. Olson, and R. Hoekstra, Phys. Rev. A **85**, 022712 (2012).
[21] M. J. J. Vrakking, Rev. Sci. Instrum. **72**, 4084 (2001).
[22] J. G. Kircz, R. Morgenstern, and G. Nienhuis, Phys. Rev. Lett. **48**, 610 (1982).
[23] H. A. J. Meijer, Ph.D. thesis, Rijksuniversiteit Utrecht, 1988.
[24] A. E. S. Green, D. L. Sellin, and A. S. Zachor, Phys. Rev. **184**, 1 (1969).
[25] R. H. Garvey, C. H. Jackman, and A. E. S. Green, Phys. Rev. A **12**, 1144 (1975).
[26] R. L. Becker and A. D. McKellar, J. Phys. B **17**, 3923 (1984).
[27] S. Knoop, M. Keim, H. J. Lüdde, T. Kirchner, R. Morgenstern, and R. Hoekstra, J. Phys. B **38**, 3163 (2005).